

---

# Robust fuzzy sliding mode control for air supply on PEM fuel cell system

---

Zakaria Baroud\* and Atallah Benalia

LACoSERE Lab,  
Amar Telidji University,  
Laghouat, Algeria  
Email: z.baroud@lagh-univ.dz  
Email: a.benalia@lagh-univ.dz  
\*Corresponding author

Carlos Ocampo-Martinez

Institut de Robòtica i Informàtica Industrial (CSIC-UPC),  
Parc Tecnològic de Barcelona,  
C/Llorens i Artigas 4–6, 08028,  
Barcelona, Spain  
Email: cocampo@iri.upc.edu

**Abstract:** In this paper, an adaptive fuzzy sliding mode controller is employed for air supply on proton exchange membrane fuel cell (PEMFC) systems. The control objective is to adjust the oxygen excess ratio at a given set point in order to prevent oxygen starvation and damage to the fuel-cell stack. The proposed control scheme consists of two parts: a sliding mode controller (SMC) and fuzzy logic controller (FLC) with an adjustable gain factor. The SMC is used to calculate the equivalent control law and the FLC is used to approximate the control hitting law. The performance of the proposed control strategy is analysed through simulations for different load variations. The results indicated that the adaptive fuzzy sliding mode controller (AFSMC) is excellent in terms of stability and several key performance indices such as the integral squared error (ISE), the integral absolute error (IAE) and the integral time-weighted absolute error (ITAE), as well as the settling and rise times for the closed-loop control system.

**Keywords:** PEM fuel cell system; oxygen starvation; sliding mode control; fuzzy logic control; stability analysis.

**Reference** to this paper should be made as follows: Baroud, Z., Benalia, A. and Ocampo-Martinez, C. (2018) 'Robust fuzzy sliding mode control for air supply on PEM fuel cell system', *Int. J. Modelling, Identification and Control*, Vol. 29, No. 4, pp.341–351.

**Biographical notes:** Zakaria Baroud earned his License degree in Electrotechnology in 2010 and his Master's degree in Automatic in 2012 from the University of Amar Telidji. He also earned the first rank in his group in License and Master. He is currently a PhD student in the Electrical Engineering Department. His general research interests are in the areas of automatic control systems and his current research focuses on the PEM fuel cell systems modelling, observation and control.

Atallah Benalia received his Diploma of State Engineer from the Ecole Polytechnique of Algiers in 1996, DEA and PhD in Automatic Control from the University of Paris-Sud, France in 1998 and 2004, respectively. He joined the Faculty of the Technology at the University of Amar Telidji, Laghouat, Algeria in 2008 where he is currently a Professor. His research interests deal mainly with analysis and control of nonlinear systems.

Carlos Ocampo-Martinez received his Electronics Engineering degree and MSc in Industrial Automation from the National University of Colombia, Manizales in 2001 and 2003, respectively. In 2007, he received his PhD in Control Engineering from the Technical University of Catalonia, UPC. In 2007–2008, he held a postdoctoral position at the University of Newcastle, Australia and afterwards in 2008–2011 at the Spanish Research Council (CSIC), Institut de Robòtica i Informàtica Industrial (IRI), CSIC-UPC. He is currently an Associate Professor at the UPC, Automatic Control Department. Since 2014, he is also Deputy Director of the IRI. His research interests include constrained predictive control, large-scale systems and industrial applications (mainly in water and energy).

---

## 1 Introduction

The serious environmental pollution and energy crisis around the world is driving innovation on new efficient and clean energy sources such as solar, wind, geothermal and hydrogen. Fuel cells are a kind of clean energy, which produce electricity, water and heat from hydrogen and oxygen (Yousfi-Steiner et al., 2009; Baroud et al., 2017).

In particular, proton exchange membrane fuel cells (PEMFC), also called solid polymer fuel cells (SPFCs), are considered to be more developed than other types of fuel cells (Larminie et al., 2003). They are used in a wide range of applications, with advantages such as high efficiency, low weight, low pollution and low operation temperature, features that allow fast starting times in the PEMFC systems (Appleby et al., 2009). However, high expenses and short lifetime have hindered their massive utilisation in real systems so far. As a result, advanced control systems are required to improve the lifetime and avoid the detrimental degradation of the PEMFC system.

One of the main problems in PEMFC systems is the so-called oxygen starvation phenomenon during stack current variation. Then, an accurate control of the oxygen excess ratio is required to avoid oxygen starvation (Baroud et al., 2016). In this context, many control strategies have been proposed. It can be mentioned, among others, linear control methods based on model linearisation such as linear quadratic regulator (LQR), proportional integral (PI) plus static feed-forward controller are proposed in Pukrushpan et al. (2004b) and Niknezhadi et al. (2011). Kunusch et al. (2009) were the first to use second-order sliding-mode strategy for the air supply PEMFC system, see Baroud et al. (2015b) and Matraji et al. (2015). In Hao et al. (2013) and Beirami et al. (2015), different topologies of fuzzy-logic control (FLC) are proposed such as adaptive PID-based FLC, optimal PID plus fuzzy controller and feed-forward fuzzy PID. Other control strategies, as gain scheduled linear parameter-varying (LPV) control (Bianchi et al., 2014), fault tolerant unfalsified control (Bianchi et al., 2015), and optimal control (Almeida and Simoes, 2009) were also reported to control the air supply PEMFC-based systems. However, these controllers impose certain limitations over the tracking performance in the presence of system uncertainties and external disturbances. This fact has led to great interest in the development of robust control methods with respect to the aforementioned drawbacks.

The sliding mode control has been an important success in the recent years due to its robustness, finite-time convergence and order compensated dynamics (Shtessel et al., 2014). It consists of defining an appropriate sliding surface, the tracking of the desired trajectory is comprised of two phases: the reaching phase and the sliding phase,

thus, the control used in this case is composed of two parts: the first is the hitting control law which enables to reach the surface and the second is the equivalent control which allows the maintain and the slide along this surface (Edwards and Spurgeon, 1998).

The sliding mode control has been used because of its simplicity of implementation and its robustness. However, the presence of the sign function in the control law causes a phenomenon known as chattering, which can excite the high-frequency dynamics (Utkin et al., 2009). To remedy this drawback while keeping the robustness of the sliding mode approach, several solutions have been proposed that combine different control approaches with the sliding mode approach to attenuate the chattering problem (Sahamijoo et al., 2016). Among these solutions, artificial intelligence approaches are considered among the best methods, in particular fuzzy logic control (Kuo et al., 2005; Wai et al., 2007; Jie et al., 2012).

Fuzzy logic was firstly proposed by Zadeh (1965) to control plants that are difficult to model. The application of fuzzy logic in control problems was firstly introduced by Mamdani (1974). The motivation of this paper is to design a controller in such way that overcomes the external disturbances and parameter uncertainties. Here, we adopted the use of a hybrid approach by combining two robust control laws: the sliding mode control (SMC) and the fuzzy logic control (FLC) to regulate efficiently the oxygen excess ratio at a set point value. This approach used a SMC to calculate the equivalent control law and used an adaptive FLC to approximate the control hitting law. To validate the proposed controller, a reduced version of the ninth-order state-space model will be adopted, which is proposed in Suh et al. (2006).

The remainder of the paper is organised as follows. Both the mathematical model of the PEMFC air supply system and the control objective are explained in Section 2. In Section 3, modules such as the sliding mode controller (SMC), the fuzzy sliding mode controller (FSMC) and the adaptive fuzzy sliding mode controller (AFSMC) are designed, respectively. The designed control strategies are applied to the model of the PEMFC system and the simulation results for stack current changes, model uncertainties are presented in detail in Section 4. Finally, the main conclusions are drawn in Section 5.

## 2 PEMFC system model

### 2.1 Nonlinear model

The PEMFC system includes five main sub-processes: the air flow (breathing), the hydrogen flow, the humidifier, the

stack electrochemistry and the stack temperature. According to (Suh et al., 2006), it is considered that sufficient compressed hydrogen is available. In addition, it is assumed that both temperature and humidity of input reactant flows are properly regulated by dedicated local controllers, and thus the main regard is focused on the air management. Under these assumptions, a fourth-order state-space model is derived, which is a reduced version of the ninth-order model presented in Pukrushpan et al. (2004a). The model equations are summarised in equations (1) to (4). The reader may refer to Pukrushpan et al. (2004a) and Gruber et al. (2008) for further details about the mathematical expressions.

The nonlinear dynamic model is described by the following continuous-time differential equations:

$$\frac{dx_1(t)}{dt} = c_1(x_4(t) - \chi(t)) - \frac{c_3x_1(t)\alpha(t)}{c_4x_1(t) + c_5x_2(t) + c_6} - c_7d(t), \quad (1)$$

$$\frac{dx_2(t)}{dt} = c_1(x_4(t) - \chi(t)) - \frac{c_3x_2(t)\alpha(t)}{c_4x_1(t) + c_5x_2(t) + c_6}, \quad (2)$$

$$\frac{dx_3(t)}{dt} = -c_9x_3(t) - \frac{c_{10}}{x_3(t)} \left( \left( \frac{x_4(t)}{c_{14}} \right)^{c_{12}} - 1 \right) W_{cp}(t) + c_{13}u(t), \quad (3)$$

$$\frac{dx_4(t)}{dt} = c_{14} \left( 1 + \left( \frac{x_4(t)}{c_{11}} \right)^{c_{12}} - 1 \right) W_{cp}(t) - c_{16}(x_4(t) - \chi(t)), \quad (4)$$

where

$$\chi(t) = x_1(t) + x_2(t) + c_2, \\ \alpha(t) = c_{17}\chi(t) \left( \frac{c_{11}}{\chi(t)} \right)^{c_{18}} \sqrt{1 - \left( \frac{c_{11}}{\chi(t)} \right)^{c_{12}}},$$

The coefficients  $c_i$ , for  $\{i = 1, \dots, 24\}$ , are defined in Table 1 in Appendix A. The vector of states  $x \in \mathbb{R}^4$  is associated to the partial pressure of oxygen and nitrogen in the cathode channel, the rotational speed of the motor shaft in the compressor and the air pressure in the supply manifold, respectively. The control input  $u(t) \in \mathbb{R}$ , as shown in Figure 1, is the compressor motor voltage  $v_{cm}(t)$ , which allows the manipulation of the air feed and, as a consequence, the oxygen supply to the fuel-cell stack. The measurable external bounded disturbance input  $d(t) \in \mathbb{R}$  is the stack current  $I_{st}(t)$ . The air flow rate through the compressor  $W_{cp}(t)$  depends on the rotational speed of the motor shaft in the compressor and the air pressure in the supply manifold, which has been approximated with the following expression.

$$W_{cp}(t) = \frac{W_{cp}^{\max} x_3(t)}{x_3^{\max}} \left( 1 - e^{-r \left( \frac{\kappa + \frac{x_3^2(t)}{q} - x_4(t)}{\kappa + \frac{x_3^2(t)}{q} - x_4^{\min}} \right)} \right), \quad (5)$$

with  $r = 15$ ,  $q = 462.25 \text{ rad}^2/(\text{s}^2\text{Pa})$ ,  $x_3^{\max} = 11500 \text{ rad/s}$ ,  $x_4^{\min} = 50000 \text{ Pa}$ ,  $\kappa = 10^5 \text{ Pa}$  and  $W_{cp}^{\max} = 0.0975 \text{ Kg/s}$ .

Moreover, the performance variables  $z(t) \in \mathbb{R}^2$ , with  $z_1(t)$  as net power and  $z_2(t)$  as oxygen excess ratio, are given by

$$z_1(t) = V_{st}(t)d(t) - c_{21}u(t)(u(t) - c_{22}x_3(t)), \quad (6)$$

$$z_2(t) = \frac{c_{23}(x_4(t) - \chi(t))}{c_{24}d(t)}. \quad (7)$$

In order to avoid repetition, the expression of  $V_{st}(t)$  is detailed in Pukrushpan et al. (2004a) and Gruber et al. (2008).

**Figure 1** Fuel cell system scheme (see online version for colours)

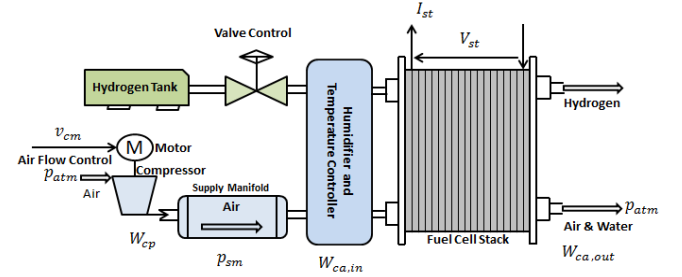
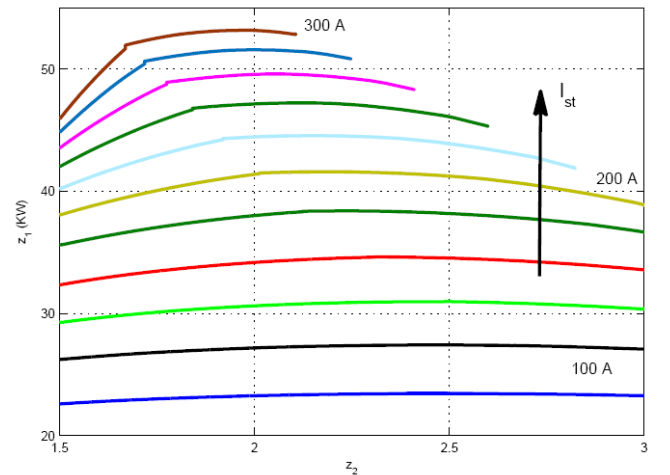


**Figure 2** The  $z_2$  performance curve for different stack currents (see online version for colours)



## 2.2 Control objective

The main control objective for the PEMFC system is to regulate the oxygen excess ratio  $z_2$ , which is defined also by the amount of oxygen provided, denoted by  $W_{O_2,in}$  and the amount of oxygen reacted, denoted as  $W_{O_2,rc}$ .

If the value of  $z_2$  is quite low, even though higher than 1, it is likely to cause *oxygen starvation*. This phenomenon can

cause a short circuit and a hot spot on the surface of the fuel-cell membrane. On the other hand, higher values of  $z_2$  will drive the compressor motor to consume more power and, therefore, towards lower efficiency operating conditions. As a result, it is necessary to state the optimal value of  $z_2$  that maximises the net power  $z_1$ . The relation between the oxygen excess ratio and the net power for different stack currents is called the performance curve (see Figure 2). It can be seen from Figure 2 that the maximum net power  $z_1$  is achieved at an oxygen excess ratio  $z_2$  between 1.9 and 2.5 for stack current variations between 100–300 A. However, in order to get the best compromise between safety and efficiency, it is necessary to regulate  $z_2$  around an optimal value  $z_{2,opt} = 2.05$  as discussed in Kunusch et al. (2009).

### 3 SMC, FSMC and AFSMC designs

To meet the above control requirements, an efficient control is required to keep the oxygen excess ratio at its optimum value. In this section, fuzzy sliding mode control is discussed.

#### 3.1 Sliding mode controller

Collecting (1) in a unique state-space representation, yields the form:

$$\dot{x}(t) = f(x) + gu(t) + \phi d(t),$$

$$= \begin{bmatrix} f_1(x_1, x_2, x_4) \\ f_2(x_1, x_2, x_4) \\ f_3(x_3, x_4) \\ f_4(x_1, x_2, x_3, x_4) \end{bmatrix} + \begin{bmatrix} 0 \\ 0 \\ c_{13} \\ 0 \end{bmatrix} u(t) - \begin{bmatrix} -c_7 \\ 0 \\ 0 \\ 0 \end{bmatrix} d(t), \quad (8)$$

The task is to force in finite time the current value of oxygen excess ratio,  $z_2(t)$ , to follow its set point value,  $z_{2,opt}$  by means of an appropriate control  $u \in \mathbb{R}$ . Hence, the tracking error is defined as follows:

$$e(t) = z_2(t) - z_{2,opt}, \quad (9)$$

To design a first-order sliding mode controller, it is worth to noting that the system relative degree must be equal to one with respect to the sliding surface, then a sliding surface is defined as:

$$s(t) = \dot{e}(t) + \lambda e(t),$$

$$= \frac{c_{23}}{c_{24}} \left[ (x_4(t) - \chi(t)) (-\dot{\phi}(t)c_{16} - c_1 - c_8) \right. \\ \left. + \dot{\phi}(t)W_{cp}(t) + \frac{c_3\alpha(t)(x_1(t) + x_2(t))}{c_4x_1(t) + c_5x_2(t) + c_6} + c_7d(t) \right] \\ - \left[ (x_4(t) - \chi(t)) \frac{\dot{d}(t)}{d(t)} \right] \\ + \lambda \frac{c_{23}}{c_{24}d(t)} \left[ (x_4(t) - \chi(t)) - z_{2,opt} \right], \quad (10)$$

where  $\phi_1(t) = c_{14} \left( 1 + \left( c_{15} \left( \frac{x_4(t)}{c_{11}} \right)^{c_{12}} - 1 \right) \right)$  and the parameter  $\lambda$  must satisfy the Hurwitz condition  $\lambda > 0$ .

Differentiating equation (10) with respect to time, yields:

$$\dot{s}(t) = \frac{\partial s}{\partial x} \dot{x}(t) + \frac{\partial s}{\partial d} \dot{d}(t) + \frac{\partial s}{\partial \dot{d}} \ddot{d}(t)$$

$$= \frac{\partial s}{\partial x} [f(x) + c_{13}u(t) - c_7d(t)]$$

$$+ \frac{\partial s}{\partial d} \dot{d}(t) + \frac{\partial s}{\partial \dot{d}} \ddot{d}(t) \quad (11)$$

$$= \frac{\partial s}{\partial x} f(x) + \frac{\partial s}{\partial x_3} c_{13}u(t) - \frac{\partial s}{\partial x_1} c_1d(t)$$

$$+ \frac{\partial s}{\partial d} \dot{d}(t) + \frac{\partial s}{\partial \dot{d}} \ddot{d}(t) + \frac{\partial s}{\partial \ddot{d}} \dddot{d}(t)$$

$$= \Psi(x, d, \dot{d}, \ddot{d}) + \Phi(x)u(t).$$

Due to readability reasons, the complete expressions of  $\Psi(x, d, \dot{d}, \ddot{d})$  and  $\Phi(x)$  are detailed in Appendix B.

The functions  $\Psi(x, d, \dot{d}, \ddot{d})$  and  $\Phi(x)$  can be globally bounded as follows:

$$0 < B_m \leq \Psi(x, d, \dot{d}, \ddot{d}) \leq B_M \quad (12)$$

$$|\Phi(x)| \leq \Theta \quad (13)$$

Once the bounds have been determined, the equivalent control signal  $u_{eq}(t)$ , which is the continuous control function required to maintain the sliding phase (Utkin et al., 2009), is the solution to:

$$\dot{s}(t) = \Psi(x, d, \dot{d}, \ddot{d}) + \Phi(x)u(t) = 0, \quad (14)$$

And then, provided  $\Phi(x)$  is non-singular, from equation (14) yields:

$$u_{eq}(t) = -(\Phi(x))^{-1} \Psi(x, d, \dot{d}, \ddot{d}). \quad (15)$$

The second stage of the design procedure is selection of the hitting control law,  $u_h$ , which is the discontinuous control required to converge the sliding surface towards zero. Therefore, a candidate Lyapunov function is defined as:

$$V(t) = \frac{1}{2} s^2(t), \quad (16)$$

Then, the derivative of  $V(t)$  along the system trajectories is of the form:

$$\dot{V}(t) = s(t) \left[ \Psi(x, d, \dot{d}, \ddot{d}) + \Phi(x)(u_{eq}(t) + u_h(t)) \right] \\ = \Phi(x)s(t)u_h(t) \quad (17)$$

The following condition must be satisfied to guarantee that the system will translate from the reaching phase to the sliding phase:

$$\dot{V}(t) = s(t)\dot{s}(t) < 0 \quad (18)$$

If equation (18) holds, then a discontinuous control law can be selected as:

$$u_h(t) = -K \operatorname{sgn}(s(t)), \quad (19)$$

where  $K$  is a positive constant and the function  $\operatorname{sgn}(s(t))$  is defined by:

$$\operatorname{sgn}(s(t)) = \begin{cases} 1 & \text{for } s(t) > 0, \\ 0 & \text{for } s(t) = 0, \\ -1 & \text{for } s(t) < 0, \end{cases} \quad (20)$$

The overall sliding mode control law becomes:

$$u(t) = u_{eq}(t) + u_h(t). \quad (21)$$

The presence of the sign function in the control law causes a phenomenon of chattering, which can excite high frequencies and some nonlinearity can not be modelled (Utkin et al., 2009). For the purpose of eliminating such phenomenon a FSMC system is used to approximate the hitting control law in equation (19) and ensures a smoother and less restrictive control for the system in the following subsection.

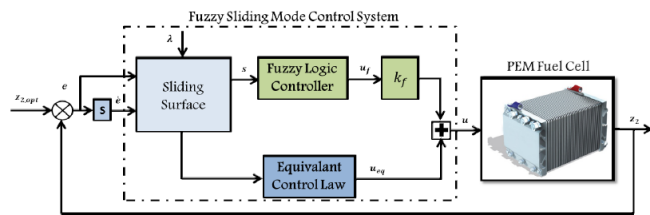
### 3.2 Fuzzy sliding mode controller

Fuzzy logic is one of the most versatile control techniques due to its simplicity, efficiency and robustness against the system dynamics variation. The fuzzy logic controller design does not require the precise information of system. There are three main parts in the fuzzy systems (Baroud et al., 2016):

- Fuzzification interface converts a crisp input to a fuzzy value by using fuzzy sets.
- Rule base and inference system generates a result for each suitable rule, then combines the results of the rules.
- Defuzzification interface converts the combined result back into a specific control output value.

The structure of the closed-loop fuzzy sliding mode control system is shown in Figure 3. It contains an equivalent control part and a fuzzy logic control part. The equivalent control law,  $u_{eq}$ , is the same as that in equation (15) and the fuzzy hitting control law,  $u_f$ , is determined by the normalised sliding variable  $s(t)$ .

**Figure 3** Closed-loop fuzzy sliding mode control system (see online version for colours)



The sliding surface  $s(t)$  is the input linguistic variable of the FLC and the fuzzy hitting control law,  $u_f$ , is the output

linguistic variable. The fuzzy subsets of input and output are expressed as *negative big* (NB), *negative medium* (NM), *negative small* (NS), *zero* (ZE), *positive big* (PB), *positive medium* (PM) and *positive small* (PS). The membership functions of input and output are respectively shown in Figures 5(a) and 5(b). The fuzzy linguistic rules of the FLC are described as:

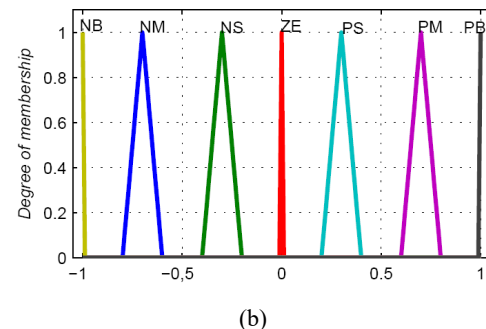
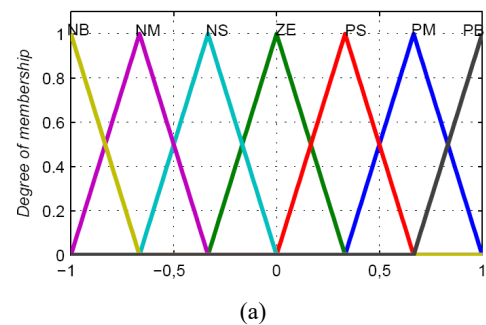
- Rule 1 IF  $s$  is PB, then  $u_f$  is NB
- Rule 2 IF  $s$  is PM, then  $u_f$  is NM
- Rule 3 IF  $s$  is PS, then  $u_f$  is NS
- Rule 4 IF  $s$  is ZE, then  $u_f$  is ZE
- Rule 5 IF  $s$  is NS, then  $u_f$  is PS
- Rule 6 IF  $s$  is NM, then  $u_f$  is PM
- Rule 7 IF  $s$  is NB, then  $u_f$  is PB.

The FLC adopted in this paper considers product-sum as the inference method, weighted average as the defuzzification method and triangular-shaped as the membership functions for the input and singleton for the output. Then, the fuzzy hitting control of the FLC is formed by weighting each functions in the output by its respective maximum membership values as follows:

$$u_f = \frac{\sum_{i=1}^7 \mu(u_{fi}) u_{fi}}{\sum_{i=1}^7 \mu(u_{fi})}, \quad (22)$$

where  $\mu(u_{fi})$  is the central value of fuzzy set at the  $i^{\text{th}}$  rule and  $u_{fi}$  is the maximum output membership value.

**Figure 4** Membership functions, (a)  $s$  (b)  $u_f$  (see online version for colours)



The overall FSMC can be represented as:

$$u(t) = u_{eq}(t) + k_f u_f(t), \quad (23)$$

where  $k_f$  is the normalisation factor of the output variable.

### 3.2.1 Stability analysis

To verify the stability property of the proposed FSMC, direct Lyapunov stability approach is employed. Taking the time derivative of the Lyapunov function in equation (16), yields

$$\begin{aligned} \dot{V}(t) &= s(t)\dot{s}(t) \\ &= s(t) \left( \frac{\partial s}{\partial x} f(x) + \frac{\partial s}{\partial x_3} c_{13} u(t) - \frac{\partial s}{\partial x_1} c_1 d(t) + \frac{\partial s}{\partial d} \dot{d} + \frac{\partial s}{\partial d} \dot{d}(t) \right) \\ &= s(t) \left( \frac{\partial s}{\partial x} f(x) + \frac{\partial s}{\partial x_3} c_{13} (u_{eq}(t) + k_f u_f(t)) \right. \\ &\quad \left. - \frac{\partial s}{\partial x_1} c_1 d(t) + \frac{\partial s}{\partial d} \dot{d}(t) + \frac{\partial s}{\partial d} \dot{d}(t) \right) \\ &= s(t) k_f u_f(t) \leq -k_f |s(t)|. \end{aligned} \quad (24)$$

Hence, the asymptotic stability condition  $\dot{V}(t) = s(t)\dot{s}(t) < 0$  is satisfied.

### 3.3 Adaptive fuzzy sliding mode controller

An adaptive fuzzy sliding mode control is proposed to enhance the dynamic and the steady-state performance of oxygen excess ratio regulation. The structure of the closed-loop adaptive fuzzy sliding mode control system, which is illustrated in Figure 5, is an extension of fuzzy sliding mode control system discussed in Section 3.2. The overall control consists of an equivalent control part and a fuzzy logic control part with an adjustable gain factor  $k_{af}$ . The overall adaptive fuzzy sliding mode control is defined as:

$$u(t) = u_{eq}(t) + k_{af} u_f(t), \quad (25)$$

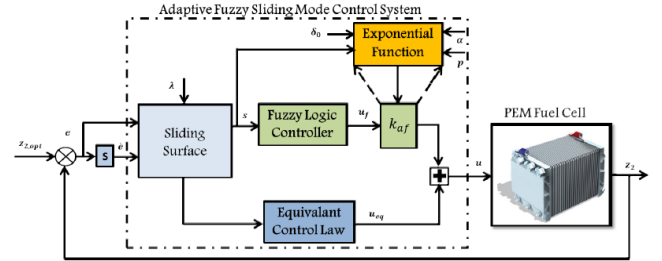
where the equivalent control,  $u_{eq}(t)$ , and the FSMC,  $u_f(t)$ , are the same that presented in Section 3.2.  $k_{af}$  is the adaptive gain factor, which is updated online, depends strongly on the sliding surface. The adaptive gain factor is formulated according to the sliding surface with the following strategy: if the output value of the system,  $z_2$ , is moving fast close to its set point, i.e., when the system approaches the sliding surface,  $k_{af}$  needs to be regularly decreases in order to limit possible large overshoot and/or undershoot. Similarly, if the output value of the system,  $z_2(t)$ , is rapidly moving away from the set point, i.e., when the system is not close to the sliding surface,  $k_{af}$  needs to be increased to reach the sliding surface promptly. Thus, the adaptive gain factor can be calculated using the following exponential relation as in Fallaha et al. (2011):

$$k_{af} = \frac{k_f}{N(s)}, \quad k_f > 0, \quad (26)$$

$$N(s) = \delta_0 + (1 - \delta_0) e^{-\alpha|s|^p} \quad (27)$$

where  $\delta_0$  is a strictly positive offset value that is less than one,  $\alpha$  and  $p$  are strictly positive values.  $k_f$  is also positive value that will bring an appropriate variations in  $k_{af}$ . And concerning the stability issue, equation (26) will not affect the stability of the system because the value of  $N(s)$  is always strictly positive.

**Figure 5** Closed-loop adaptive fuzzy sliding mode control system (see online version for colours)



The performance indices of the PEMFC control system include the integral squared error (ISE):

$$ISE = \int_0^{t_f} |e(t)|^2 dt, \quad (28)$$

The integral absolute error (IAE):

$$IAE = \int_0^{t_f} |e(t)| dt, \quad (29)$$

And the integral time-weighted absolute error (ITAE):

$$ITAE = \int_0^{t_f} |e(t)| dt. \quad (30)$$

## 4 Simulation results and analysis

To verify the performance, the robustness and the efficiency of the proposed control strategies, detailed simulations are performed and analysed. Simulations are divided into two groups: performance results and sensitivity analysis. The numerical parameters used in the simulation are given in Table 1 in Appendix A. The initial states values are chosen as:

$$x(0) = [11104 \text{ Pa} \quad 83893 \text{ Pa} \quad 5100 \text{ rad/s} \quad 148000 \text{ Pa}]^T. \quad (31)$$

The main aim to design these controllers is to regulate the oxygen excess ratio at a set point value, which is assumed equal to 2.05. With this set point, it can be assured that the PEMFC system works within the range of its maximum net power for each load variation while the oxygen starvation is avoided. The simulation of the proposed control system is carried out using the MATLAB/Simulink package and the control parameters are given as:

$$\delta_0 = 0.5, \alpha = 9, p = 4 \text{ and } k_f = 15.$$

#### 4.1 Performance results

This subsection shows a comparison study between the control strategies presented in this paper, i.e., sliding mode, fuzzy sliding mode and adaptive fuzzy sliding mode. The dynamic behaviour of  $z_2$  under different stack current variation, using SMC, FSMC and AFSMC control strategies, is shown in Figure 7. The stack current, as depicted in Figure 6, decreases from 260A to 180A at  $t = 8$  s. Next, after 7 s, it increases by 140A to reach 320 A. After 20 s, the current falls to 240 A. Finally, at time  $t = 25$  s, it increases again from 230A to 270 A. It can be seen from Figure 7 that all the applied control strategies adjust  $z_2$  at the set point value with a satisfactory tracking performance.

**Figure 6** Stack current variation

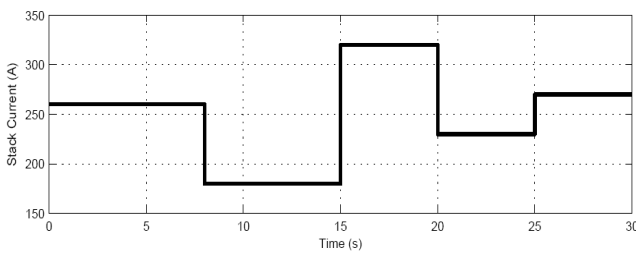
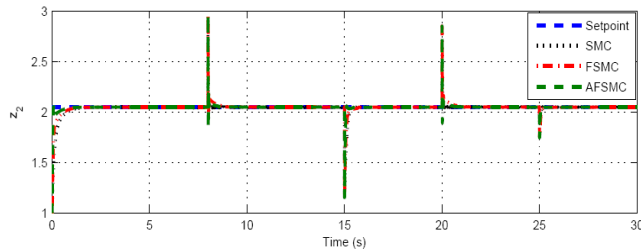


**Figure 7** Response of oxygen excess ratio for different control strategies (see online version for colours)



Figures 9(a) and 9(b) present the zoomed plot of  $z_2$  when the stack current is decreased from 260A to 180A (at  $t = 8$  s) and when the stack current is increased from 230A to 270A (at  $t = 25$  s), respectively. In the second case, the oxygen excess ratio decreases, as shown in Figure 9(b), due to the depletion of oxygen at the cathode side. This fact caused an important drop of the stack voltage, as shown in Figure 9. An inverse case is shown in Figure 9(a) at  $t = 8$  s. According to the zoomed plot of  $z_2$  [Figures 9(a) and 9(b)], it is found that the AFSMC exhibits a faster time response compared to the other control strategies. As it can be seen in Figure 7 and Table 1, that the AFSM controller reduces the rise time and the settling time of tuning  $z_2$  during the transient step changes of stack current,  $d$ , with respect to the SMC and FSMC controllers. The results in Table 1 show also, in terms of several performance indices including: the ISE, the IAE and the ITAE, that the proposed control strategy performs much better than the SMC and FSMC control strategies.

To further show the effectiveness of the proposed control strategy (AFSMC) on the PEMFC systems, changes of  $z_{2,opt}$  are considered, rising up from 2.05 to 3 at  $t = 20$  s and then, falling to 2.05 at  $t = 30$  s. Simulation results show in Figure 10 that  $z_2$  suitably and accurately tracks  $z_{2,opt}$  in the presence of stack current variation.

**Figure 8** The zoomed plot of oxygen excess ratio variations at (a)  $t = 8$  s and (b)  $t = 25$  s (see online version for colours)

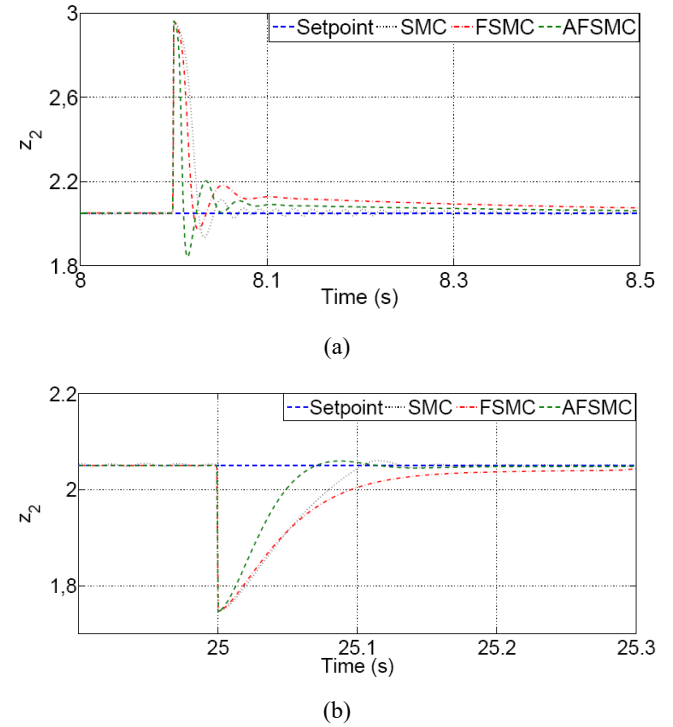
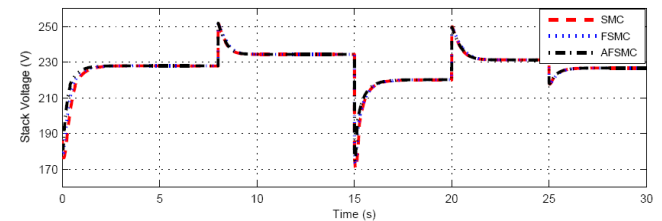


**Figure 9** Stack voltage variation for different control strategies (see online version for colours)



#### 4.2 Sensitivity analysis

In order to test the robustness of the AFSM controller in the presence of parameter uncertainty, a small variation can be applied to the combined inertia of the compressor and the motor ( $J_{cp}$ ), which is related to the capacity of the air to be supplied from the compressor. This parameter uncertainty appears at the time interval  $t = [10, 20]$  s, as shown in Figure 12(b). It can be seen from Figure 12(a) that the AFSM controller exhibits a proper effect over this uncertainty. The zoomed plot is shown in Figure 12(c), where the transient response of  $z_2$  can be seen at  $t = 15$  s.

**Table 1** Performance index comparison and time domain specifications

Controllers	ISE	IAE	ITAE	Rise time (s)	Settling time (5%) (s)
SMC	0.1836	0.4169	3.2609	0.037	0.03
FSMC	0.1254	0.3383	3.2017	0.052	0.045
AFSMC	0.073	0.1765	1.7023	0.011	0.01

**Figure 10** Response of oxygen excess ratio at varied values (see online version for colours)

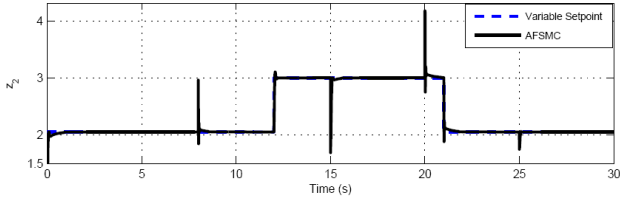
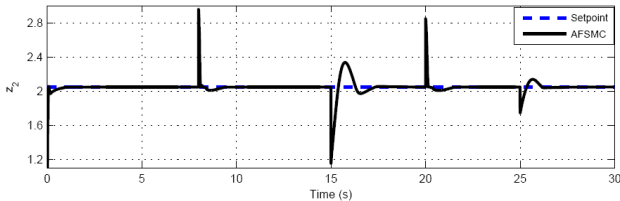
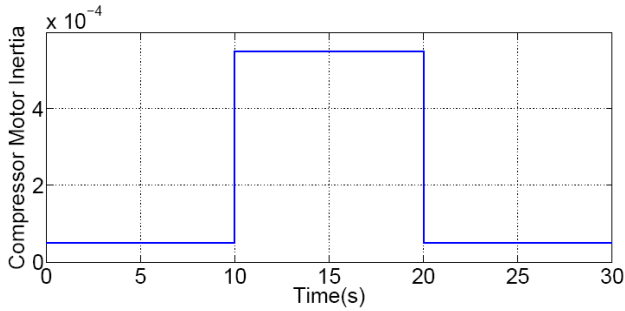


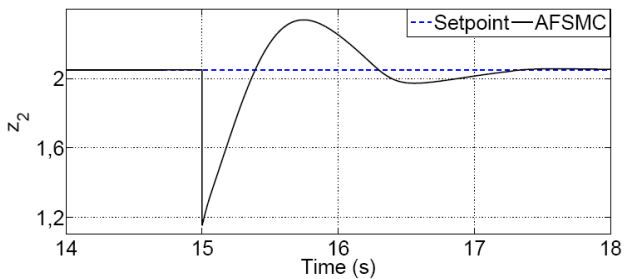
**Figure 11** Sensitivity analysis, (a)  $z_2$  considering compressor motor inertia variation (b) compressor motor inertia variation (c) zoomed plot of  $z_2$  at  $t = 15$  s (see online version for colours)



(a)



(b)



(c)

## 5 Conclusions

In this paper, a reduced PEMFC system model is proposed, which presents cathode mass flow transients. Based on this model, an adaptive fuzzy sliding mode controller is designed to regulate the oxygen excess ratio during fast current transitions. The proposed strategy is an integration of two parts with an adjustable gain: sliding mode control and fuzzy logic control. Simulation results show that the adaptive fuzzy sliding mode controller can provide the best performance with respect to SMC and FSMC strategies. This is due to the combination of the advantages of SMC and FLC. As future research, the applicability of the AFSMC will be confirmed in a sensorless control scheme.

## References

- Almeida, P. and Simoes, M. (2009) 'Neural optimal control of PEM fuel cells with parametric CMAC networks', *IEEE Transactions on Industry Applications*, Vol. 41, No. 1, pp.237–245.
- Appleby, A.J. (2009) 'Fuel cells overview introduction', in Garche, J. (Ed.): *Encyclopedia of Electrochemical Power Sources*, Elsevier, The Center of Electrochemical Systems and Hydrogen Research, Texas, USA.
- Baroud, Z., Benalia, A. and Ocampo-Martinez, C. (2016) 'Air flow regulation in fuel cells: an efficient design of hybrid fuzzy-PID control', in *Electrotehnica, Electronica, Automatica (EEA)*, Vol. 64, No. 4, pp.28–32.
- Baroud, Z., Benmiloud, M. and Benalia, A. (2015a) 'Fuzzy self-tuning PID controller for air supply on a PEM fuel cell system', in *4th International Conference on Electrical Engineering (ICEE)*, pp.1–4.
- Baroud, Z., Benmiloud, M. and Benalia, A. (2015b) 'Sliding mode controller for breathing subsystem on a PEM fuel cell system', in *3rd International Conference on, Control and Engineering Information Technology (CEIT)*, pp.1–6.
- Baroud, Z., Benmiloud, M., Benalia, A. and Ocampo-Martinez, C. (2017) 'Novel hybrid fuzzy-PID control scheme for air supply in PEM fuel cell-based systems', *International Journal of Hydrogen Energy*, Vol. 42, No. 15, pp.10435–10447.
- Beirami, H., Shabestari, A. and Zerafat, M. (2015) 'Optimal PID plus fuzzy controller design for a PEM fuel cell air feed system using the self-adaptive differential evolution algorithm', *International Journal of Hydrogen Energy*, Vol. 40, No. 30, pp.9422–9434.
- Bianchi, F., Kunsch, C., Ocampo-Martinez, C. and Sánchez Peña, R. (2014) 'A gain-scheduled LPV control for oxygen stoichiometry regulation in PEM fuel cell systems', *IEEE Transactions on Control Systems Technology*, Vol. 22, No. 5, pp.1837–1844.
- Bianchi, F., Kunsch, C., Ocampo-Martinez, C. and Sánchez Peña, R. (2015) 'Fault-tolerant unfalsified control for PEM fuel cell systems', *IEEE Transactions on Energy Conversion*, Vol. 30, No. 1, pp.307–315.
- Edwards, C. and Spurgeon, S. (1998) *Sliding Mode Control: Theory and Applications*, CRC Press, UK.

Fallaha, C.J., Saad, M., Kanaan, H.Y. and Al-Haddad, K. (2011) 'Sliding-mode robot control with exponential reaching law', *IEEE Transactions on Industrial Electronics*, Vol. 58, No. 2, pp.600–610.

Gruber, J., Bordons, C. and Dorado, F. (2008) 'Nonlinear control of the air feed of a fuel cell', in *American Control Conference*, pp.1121–1126.

Hao, X., Zhang, H., An, A., Liu, X. and Chen, L. (2013) *Fuzzy Double Model Control for Air Supply on a PEM Fuel Cell System*, Vol. 335, pp.392–400, Springer, Berlin, Heidelberg.

Jie, S., Yong, Z. and Chengliang, Y. (2012) 'Longitudinal brake control of hybrid electric bus using adaptive fuzzy sliding mode control', *International Journal of Modelling, Identification and Control*, Vol. 15, No. 3, pp.147–155.

Kunusch, C., Puleston, P., Mayosky, M. and Riera, J. (2009) 'Sliding mode strategy for PEM fuel cells stacks breathing control using a super-twisting algorithm', *IEEE Transactions on Control Systems Technology*, Vol. 17, No. 1, pp.167–174.

Kuo, C.L., Li, T.H. and Guo, N.R. (2005) 'Design of a novel fuzzy sliding-mode control for magnetic ball levitation system', *Journal of Intelligent and Robotic Systems*, Vol. 42, No. 3, pp.295–316.

Larminie, J., Dicks, A. and McDonald, M.S. (2003) *Fuel Cell Systems Explained*, Vol. 2, Wiley, New York.

Mamdani, E. (1974) 'Application of fuzzy algorithms for control of simple dynamic plant', *Proceedings of the Institution of Electrical Engineers*, Vol. 121, No. 3, pp.1585–1588.

Matraji, I., Ahmed, F.S., Laghrouche, S. and Wack, M. (2015) 'Comparison of robust and adaptive second order sliding mode control in PEMFC air-feed systems', *International Journal of Hydrogen Energy*, Vol. 40, No. 30, pp.9491–9504.

Niknezhadi, A., Allué-Fantova, M., Kunusch, C. and Ocampo-Martinez, C. (2011) 'Design and implementation of LQR/LQG strategies for oxygen stoichiometry control in PEM fuel cells based systems', *Journal of Power Sources*, Vol. 196, No. 9, pp.4277–4282.

Pukrushpan, J., Stefanopoulou, A. and Peng, H. (2004a) 'Fuel cell system model: fuel cell stack', in *Control of Fuel Cell Power Systems*, Springer, London.

Pukrushpan, J.T., Stefanopoulou, A. and Peng, H. (2004b) 'Control of fuel cell breathing', *Control Systems, IEEE*, Vol. 24, No. 2, pp.30–46.

Sahamijoo, A., Piltan, F., Mazloom, M.H., Avazpour, M.R., Ghiasi, H. and Sulaiman, N.B. (2016) 'Methodologies of chattering attenuation in sliding mode controller', *International Journal of Hybrid Information Technology*, Vol. 9, No. 2, pp.11–36.

Shtessel, Y., Christopher, E., Fridman, L. and Levant, A. (2014) *Sliding Mode Control and Observation*, Springer, Suisse.

Suh, K.W. (2006) *Modeling, Analysis and Control of Fuel Cell Hybrid Power Systems*, PhD thesis.

Utkin, V., Guldner, J. and Shi, J. (2009) *Sliding Mode Control in Electro-Mechanical Systems*, Vol. 34, CRC Press, UK.

Wai, R.J. (2007) 'Fuzzy sliding-mode control using adaptive tuning technique', *IEEE Transactions on Industrial Electronics*, Vol. 54, No. 1, pp.586–594.

Yousfi-Steiner, N., Moçotéguy, P., Candusso, D. and Hissel, D. (2009) 'A review on polymer electrolyte membrane fuel cell catalyst degradation and starvation issues: causes, consequences and diagnostic for mitigation', *Journal of Power Sources*, Vol. 194, No. 1, pp.130–145.

Zadeh, L. (1965) 'Fuzzy sets', *Information and Control*, Vol. 8, No. 3, pp.338–353.

## Appendix A

### Constants and parameters of the PEMFC system

**Table A1** Constants of the PEMFC system model

$c_1 = \frac{RT_{st}k_{ca,in}}{M_{O_2}V_{ca}} \left( \frac{x_{O_2,atm}}{1 + \omega_{atm}} \right)$	$c_{15} = \frac{1}{\eta_{cp}}$
$c_2 = P_{sat}$	$c_{16} = k_{ca,in}$
$c_3 = \frac{RT_{st}}{V_{ca}}$	$c_{17} = \frac{C_D A_T}{\sqrt{RT_{st}}} \sqrt{\frac{2\gamma}{\gamma-1}}$
$c_4 = M_{O_2}$	$c_{18} = \frac{1}{\gamma}$
$c_5 = M_{N_2}$	$c_{19} = \left( \frac{2}{\gamma+1} \right)^{\frac{\gamma}{\gamma-1}}$
$c_6 = M_v P_{sat}$	$c_{20} = \frac{C_D A_T}{\sqrt{RT_{st}}} \gamma^{0.5} \left( \frac{2}{\gamma+1} \right)^{\frac{\gamma+1}{2\gamma-2}}$
$c_7 = \frac{RT_{st}n}{4FV_{ca}}$	$c_{21} = \frac{1}{R_{cm}}$
$c_8 = \frac{RT_{st}k_{ca,in}}{M_{N_2}V_{ca}} \left( \frac{1 - x_{O_2,atm}}{1 + \omega_{atm}} \right)$	$c_{22} = k_v$
$c_9 = \frac{n_{cm}k_t k_v}{J_{cp}R_{cm}}$	$c_{23} = k_{ca,in} \left( \frac{x_{O_2,atm}}{1 + \omega_{atm}} \right)$
$c_{10} = \frac{C_p T_{atm}}{J_{cp} \eta_{cp}}$	$c_{24} = \frac{nM_{O_2}}{4F}$
$c_{11} = p_{atm}$	$x_{O_2,atm} = \frac{y_{O_2,atm} M_{O_2}}{M_{a,atm}}$
$c_{12} = \frac{\gamma-1}{\gamma}$	
$c_{13} = \frac{\eta_{cm}k_t}{J_{cp}R_{cm}}$	$\omega_{atm} = \frac{M_v}{M_{a,atm}} \frac{\phi_{atm} P_{sat}}{p_{atm} - \phi_{atm} P_{sat}}$
$c_{14} = \frac{RT_{atm\gamma}}{M_{a,atm}V_{sm}}$	



$$\Phi(t, x) = \left[ \frac{c_{23}c_{14}}{c_{24}d(t)} \left( 1 + \left( c_{15} \left( \frac{x_4(t)}{c_{11}} \right)^{c_{12}} - 1 \right) \right) \alpha(t) e^{\left( \frac{-r \left( s + \frac{x_3^2(t)}{q} - x_4(t) \right)}{s + \frac{x_3^2(t)}{q} - x_4^{\min}} \right)} \right. \\ \left. \times \left[ 1 \times \left( \frac{2x_3^2(t) \left( s - x_4^{\min} + \frac{x_3^2(t)}{q} + \frac{r \left( s + \frac{x_3^2(t)}{q} - x_4(t) \right)}{q} \right)}{\left( s + \frac{x_3^2(t)}{q} - x_4^{\min} \right)} \right) \right] \right] c_{13}.$$